G. Öhlmann *et al.* (Editors), *Catalysis and Adsorption by Zeolites*
© 1991 Elsevier Science Publishers B.V., Amsterdam


# INCORPORATION OF SILICON INTO THE FRAMEWORK OF SAPO-5 STUDIED BY NMR AND IR SPECTROSCOPY

B. Zibrowius[1], E. Löffler[1], G. Finger[1], E. Sonntag[2], M. Hunger[3] and J. Kornatowski[4]

[1]Central Institute of Physical Chemistry and [2]Central Institute of Inorganic Chemistry of the Academy of Sciences of the GDR, Rudower Chaussee 5, Berlin, DDR-1199 (German Democratic Republic)

[3]Department of Physics, Karl-Marx-University Leipzig, Linnéstr. 5, Leipzig, DDR-7010 (German Democratic Republic)

[4]Institute of Chemistry, Nicolaus Copernicus University, Gagarina 7, 87-100 Torun (Poland)

## SUMMARY

SAPO-5 was synthesized from starting gels covering a broad range of composition. The incorporation of silicon into the AFI framework was studied by multinuclear MAS NMR and IR spectroscopy. It was found that the gel composition determines the morphology of the crystals, but only slightly influences the amount of silicon incorporated. An upper limit for the incorporation of isolated silicon atoms can be expected.

## INTRODUCTION

Crystalline silicoaluminophosphate molecular sieves (SAPOs) are novel microporous solids which can be considered as derivatives from the corresponding aluminophosphates by isomorphous substitution (ref. 1). Different mechanisms for this substitution are discussed. Only in the case of an incorporation of monomeric silicon on phosphorus sites (i.e. the silicon atoms are bonded via oxygen to four adjacent aluminium atoms), the calcination of the as-synthesized SAPO generates one Bronsted acidic site per one silicon atom incorporated. Therefore, not only the overall content, but also the type of silicon incorporation determines the catalytic activity of SAPOs.

The goal of our work was to investigate the influence of gel composition on the final composition of the crystals and, in particular, on the silicon incorporation into the framework of the resulting differently sized and shaped SAPO-5 crystals. Furthermore, we want to show that the combination of NMR and IR spectro-

scopy is an appropriate tool to obtain more detailed information about the samples. The present paper is a direct continuation of ref. 2. The samples were synthesized from starting gels within a broad range of composition. The solids obtained after crystallization were characterized by XRD and scanning electron microscopy and analyzed chemically. To study the silicon incorporation, solid state $^{31}P$, $^{29}Si$, $^{27}Al$ and $^{1}H$ MAS NMR as well as IR spectroscopy were applied.

## EXPERIMENTAL

### Synthesis

SAPO-5 sample were synthesized hydrothermally at 190°C starting from gels of different molar ratios of the components a $Al_2O_3$ · b $P_2O_5$ · c TEA · d $SiO_2$ · e $H_2O$ (cf. Table 2). The gels were formed applying an aluminiumoxydehydrate sol (2.35 mass% $Al_2O_3$), phosphoric acid (85 mass% $H_3PO_4$), triethylamine (TEA) acting as template, a silica sol (40 mass% $SiO_2$), and bidistilled water. The starting pH value of the gel was 3.3 ± 0.2 rising to about 7.0 after completion of the crystallization process. The obtained crystals were separated from the mother liquor and, if necessary, from some occasionally formed small amount of by-products, washed carefully and dried. Calcination was performed under air at 750°C. A more detailed description of the synthesis is given in ref. 2.

### Chemical analysis

The determination of the chemical composition of the SAPO-5 samples as given in Table 2 was carried out by wet chemical analysis using the following procedures.

After calcination at 1000°C, the powdered material was fused with sodium carbonate (fivefold excess) followed by dissolution into hydrochloric acid. For the determination of silicon, polyethylene oxide solution was used to aggregate the silicic acid. The precipitate was filtered, washed and weighed after heating at 1100°C. Then hydrofluoric acid was added to evaporate silicon dioxide. The quantity of silicon was determined on the basis of weight reduction. The filtrate was taken to quantify the residual amount of silicon dioxide by means of the molybdenum blue spectrophotometry.

The filtrate of silicic acid was taken to obtain the amounts of $Al_2O_3$ and $P_2O_5$. Aluminium was precipitated by 8-hydroxyquinoline in a weak acetic acid solution (pH = 6...7, 50°C). The oxyquinolate of aluminium was fritted, washed with little cold water and weighed as $Al(C_9H_6ON)_3$ after drying for 2 h at 135°C. Phosphate was precipitated as magnesium ammonium phosphate in a two-step procedure. The precipitate was filtered, washed and the paper subsequently ashed. After heating at 1100°C, the residue was weighed as $Mg_2P_2O_7$.

Instrumental

The $^{27}Al$, $^{29}Si$ and $^{31}P$ MAS NMR spectra were recorded on a Bruker MSL 400 spectrometer. The experimental conditions for the NMR measurements are summarized in Table 1. All spectra shown in this paper were obtained by single pulse excitation. In the case of $^{29}Si$ and $^{31}P$ MAS NMR, high-power proton decoupling was applied. The chemical shifts reported for $^{27}Al$ are not corrected for second-order quadrupole effects.

$^{1}H$ MAS NMR spectra were measured at room temperature using a Bruker MSL 300 spectrometer and a home-made magic-angle-spinning equipment that allows to spin sealed glass ampoules. The total concentration of OH groups in the activated samples was determined by comparing the line intensity with that of a standard.

TABLE 1
Experimental conditions for MAS NMR measurements.

| nucleus | resonance frequency /MHz | pulse duration /µs | flip angle | repetition time /s | no. of scans | MAS frequ. /kHz | reference |
|---|---|---|---|---|---|---|---|
| $^{1}H$ | 300.0 | 4.0 | $\pi/2$ | 10.0 | 400 | 2.5 | TMS |
| $^{27}Al$ | 104.2 | 0.6 | $\pi/12$ | 0.5 | 800 | 5.1 | $Al(H_2O)_6^{3+}$ |
| $^{29}Si$ | 79.5 | 2.5 | $\pi/4$ | 5.0 | ≥2000 | 4.2 | TMS |
| $^{31}P$ | 161.9 | 3.0 | $\pi/2$ | ≥15.0 | 64 | 4.8 | $H_3PO_4$(85%) |

For the $^{1}H$ MAS NMR measurements, the samples were pretreated in a glass tube of 5.5 mm inner diameter with a 10 mm bed-depth. Starting at room temperature, the samples were heated under vacuum

with a rate of 10 K/h. After keeping for 2 h at 670 K, the samples were evacuated up to a pressure below 0.01 Pa for 20 h and sealed off.

The same samples were used in DRIFT (diffuse reflectance IR Fourier transform) investigations of OH groups. In some cases an anologous pretreatment in a special vacuum cell (ref. 3) was carried out before the IR measurements. The DRIFT measurements were performed with a Fourier spectrometer IRF 180 (Centre of Scientific Instrumentations of the Academy of Sciences of the GDR) with a resolution of 4 $cm^{-1}$. An empty glass tube or a rough copper surface in the vacuum cell were employed as the standard, respectively.

## RESULTS AND DISCUSSION

By means of XRD it was proven that all samples investigated exhibit indeed AFI structure (ref. 4). The quite different morphology of the the crystals is illustrated in ref. 2: sample A in Fig. 1A, samples B and D in Figs. 2D and 4B and sample C in Fig. 4E. The chemical compositions of both the gels and the calcined samples are given in Table 2. Although the compositions of the gels cover a broad range, the composition of the SAPO-5 crystals is nearly constant.

TABLE 2

Chemical compositions of both the gels and the calcined and dehydrated samples.

| sample | gel | | | | | calcined sample | | | |
|---|---|---|---|---|---|---|---|---|---|
| | $Al_2O_3$ : | $P_2O_5$ : | $SiO_2$ : | TEA: | $H_2O$ | Al : | P : | Si | Al/(P+Si) |
| A* | 1.0 : | 1.03: | 0.25: | 1.55: | 300 | 0.506: | 0.458: | 0.036 | 1.024 |
| B | 1.0 : | 2.06: | 0.25: | 3.10: | 300 | 0.505: | 0.459: | 0.036 | 1.020 |
| C* | 1.0 : | 1.03: | 1.00: | 1.55: | 300 | 0.505: | 0.442: | 0.053 | 1.021 |
| D | 1.0 : | 2.06: | 1.00: | 3.10: | 300 | 0.498: | 0.465: | 0.037 | 0.992 |
| E* | 1.0 : | 1.18: | 0.24: | 1.72: | 450 | - | - | - | - |
| F | 1.0 : | 2.35: | 1.00: | 3.43: | 450 | - | - | - | - |

*samples containing small amounts of by-products which were separated before the NMR and IR investigations

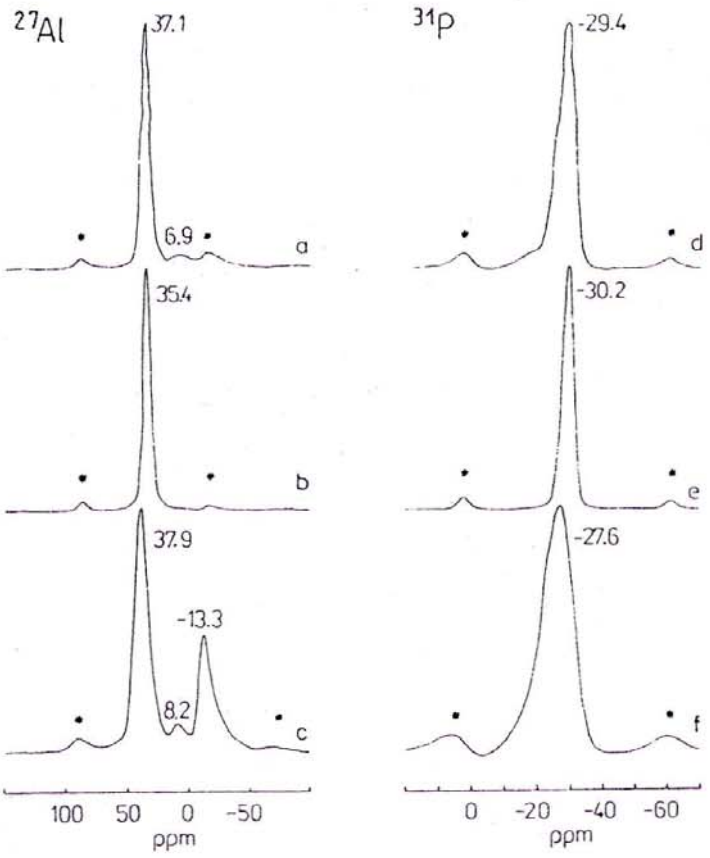


Fig. 1. $^{27}Al$ and $^{31}P$ MAS NMR spectra of SAPO-5 (sample A): (a+d) as-synthesized, (b+e) calcined and dehydrated and (c+f) calcined and rehydrated. Spinning sidebands are denoted by asterisks.

$^{27}Al$ and $^{31}P$ MAS NMR spectra of sample A are shown in Fig. 1. For both nuclei we observe only one line in the spectra of the calcined and dehydrated sample confirming the strict alternation of phosphorus and aluminium at T positions of the aluminophosphate framework (ref. 5). The line at 35.4 ppm in the $^{27}Al$ NMR spectrum has to be ascribed to tetrahedrally coordinated aluminium atoms bonded via oxygen to four phosphorus atoms, whereas the line at -30.2 ppm in the $^{31}P$ NMR spectrum corresponds to phosphorus linked with four $AlO_4$ tetrahedra (refs. 5,6).

The substitution of a part of the framework T positions by silicon is not reflected in the spectra. The single resonance line obtained for phosphorus corroborates that P-O-Si bonds are unlikely to occur (ref. 1). The different environments of the phosphorus nuclei in the case of a silicon incorporation on hypothetical aluminium T sites should be detectable in $^{31}P$ MAS NMR spectra.

The spectra in Fig. 1 also indicate that large changes in the

AFI framework occur during sample calcination and rehydration. These changes seem to be a common feature of many aluminophosphate-based materials (refs. 6-9). Comparing the spectra in Fig. 1 with those of $AlPO_4$-5, we found no influence of the silicon incorporation. The $^{27}Al$ and $^{31}P$ MAS NMR spectra of the different SAPO-5 samples are almost identical and agree with those of the silicon-free $AlPO_4$-5. Although otherwise stated in ref. 10, the intensity of the line due to octahedrally coordinated aluminium in the $^{27}Al$ MAS NMR spectrum of the calcined and rehydrated sample (-13.3 ppm in Fig. 1c) does not depend on the amount of silicon incorporated. Neither $^{27}Al$ nor $^{31}P$ MAS NMR can be used to detect or to quantify the amount of silicon incorporated into an aluminophosphate framework.

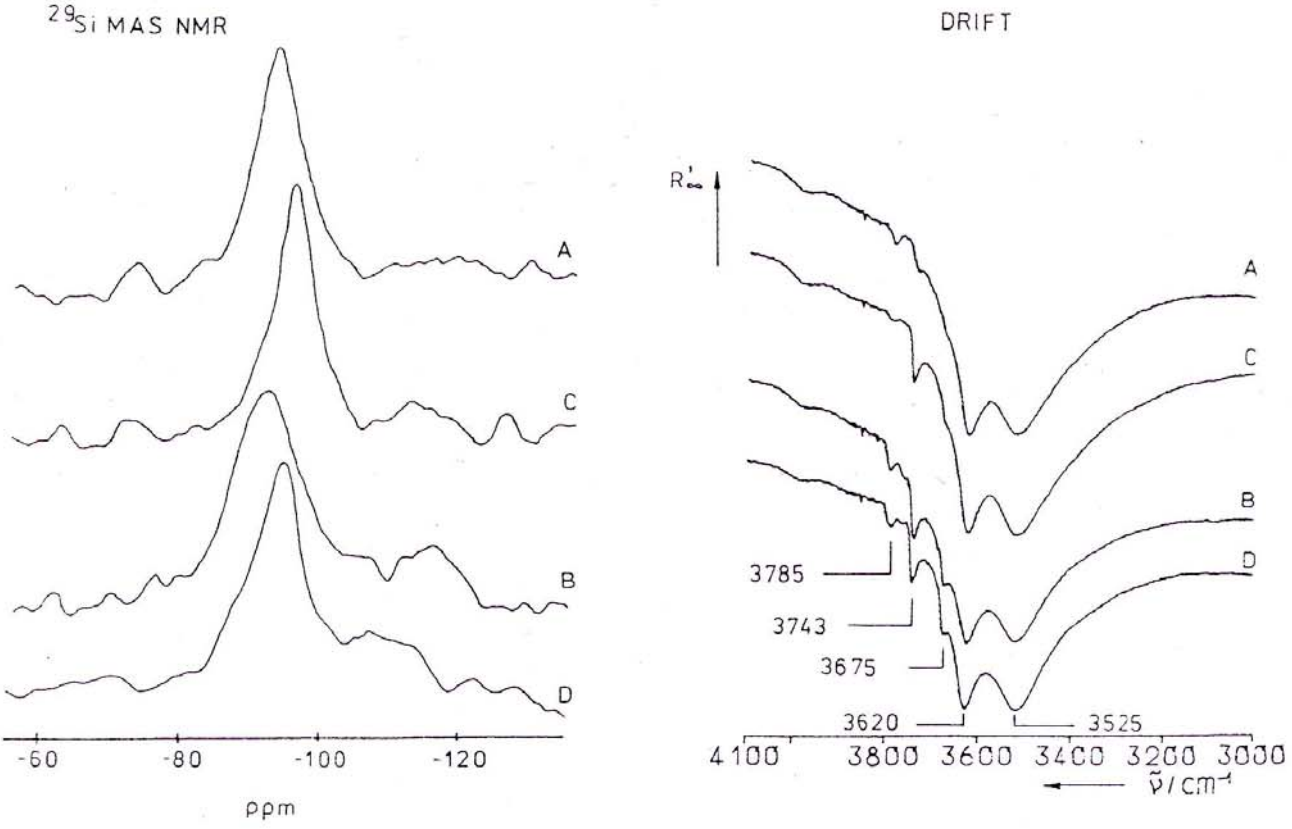


Fig. 2. $^{29}Si$ MAS NMR and DRIFT spectra of calcined and dehydrated SAPO-5. Denotation as in Table 2.

$^{29}Si$ MAS NMR is the only direct method to investigate the type of silicon incorporation. The $^{29}Si$ NMR spectra together with the corresponding diffuse reflectance IR Fourier transform spectra are shown in Fig. 2. The $^{29}Si$ NMR lines with maxima between -91 ppm and -96 ppm are ascribed to silicon atoms bonded via oxygen to

four aluminium atoms (refs. 7,11-15). Each silicon atom incorporated in this way should cause one Bronsted acidic site. A weak second signal at about -110 ppm can be seen in the case of samples B, C and D. It stems from silicon atoms bonded via oxygen to four silicon. These pure silica units may be present in silica islands within the AFI structure or in an amorphous by-product (refs. 12,13). Since we have found that the sometimes obtained by-product is in our case an aluminophosphate (vide infra), the former explanation is more likely. In line with the findings of ref. 13, an increase of the overall silicon content increases the relative intensity of the -110 ppm line, i.e. lowers the number of Bronsted acidic sites per silicon atom in the sample.

The hydroxyls generated by the silicon incorporation can be studied by both IR and $^{1}H$ MAS NMR spectroscopy. The diffuse reflectance IR Fourier transform spectra in Fig. 2 present the region of fundamental OH stretching vibrations $\nu_{0-1}$. Two bands at 3625 and 3520 $cm^{-1}$ are observed due to Bronsted acidic sites (SiOHAl groups). Corresponding to literature (refs. 16,17), we propose that these different two bands characterize undisturbed SiOHAl groups (3625 $cm^{-1}$) and SiOHAl groups interacting with lattice oxygen (3520 $cm^{-1}$). The three low intensity lines at 3785, 3745 and 3675 $cm^{-1}$ are caused by AlOH, SiOH and POH groups, respectively (ref. 17).

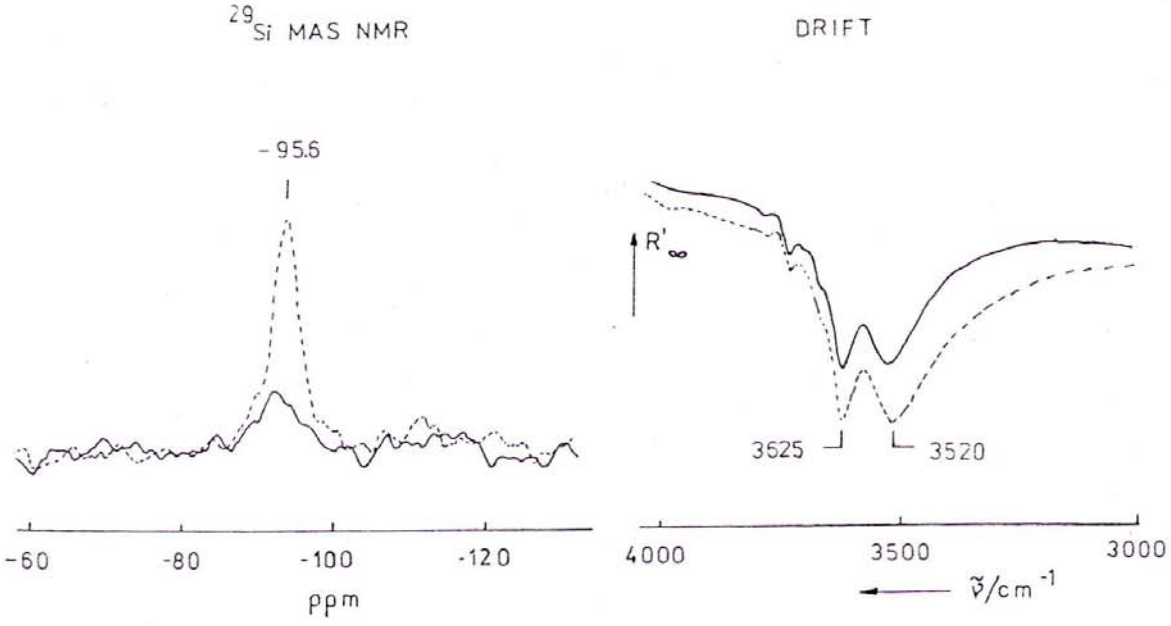


Fig. 3. $^{29}Si$ MAS NMR and DRIFT spectra of the samples E (broken lines) and F (solid lines).

As Fig. 3 shows, the sensitivities of $^{29}Si$ MAS NMR and DRIFT are rather different. The samples differ strongly in the amount of incorporated silicon due to a non-optimized synthesis procedure. In the case of sample F, there is only a weak $^{29}Si$ NMR line at -95.6 ppm characterizing the monomerically incorporated silicon, but the vibration bands of OH groups due to this type of silicon incorporation are quite intense. Hence, it can be concluded that the DRIFT spectroscopy is a very sensitive method to prove monomerically incorporated silicon.

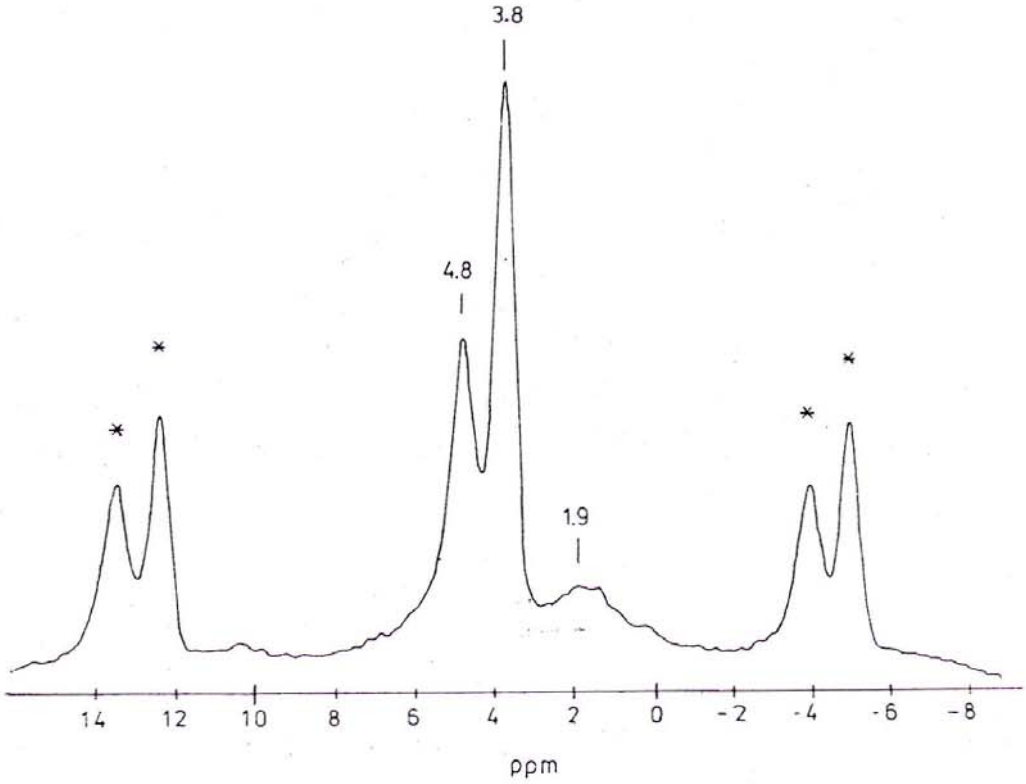


Fig. 4. $^{1}H$ MAS NMR spectrum of SAPO-5 (sample A).

IR spectroscopy always encounters difficulties in obtaining reliable quantitative data on the number of the different hydroxyls. This problem can be solved by the application of $^{1}H$ MAS NMR spectroscopy. The $^{1}H$ MAS NMR spectrum of SAPO-5 consists of three lines (Fig. 4). The lines at 4.8 and 3.8 ppm are caused by bridging SiOHAl groups and correspond to the IR bands at 3520 and 3625 $cm^{-1}$, respectively. Furthermore a broad band at 1.9 ppm is observed, which was ascribed to POH groups (ref. 11). But also terminal SiOH groups can contribute to this line. The data are summarized in Table 3. Except for sample C, the number of bridging

hydroxyls agrees well with the total number of silicon atoms present in the samples. This finding indicates an almost exclusively monomeric incorporation of the silicon and is therefore in accordance with the silicon spectra shown in Fig. 2. From the -110 ppm line present in the silicon spectra, one would assume that, except for sample A, the total number of silicon atoms should slightly exceed the number of bridging hydroxyls. Discussing these quantitative details, the fact that we are dealing with very small amounts of silicon and hydroxyls has to be considered.

TABLE 3

Concentrations of silicon atoms and hydroxyl groups.

| sample | silicon atoms[a] /$10^{20}$ $g^{-1}$ | bridging OH[b] /$10^{20}$ $g^{-1}$ | non-acidic OH[c] /$10^{20}$ $g^{-1}$ |
|---|---|---|---|
| A | 3.6 | 4.4 | 0.5 |
| B | 3.6 | 4.6 | 0.5 |
| C | 5.3 | 3.5 | 0.5 |
| D | 3.7 | 3.2 | 0.5 |
| E | - | 2.8 | 0.6 |
| F | - | 1.6 | 0.6 |

a from chemical analysis
b from the intensities of the $^1$H NMR lines at 3.8 and 4.8 ppm ($\pm 0.5 \cdot 10^{20}$ $g^{-1}$)
c from the intensity of the $^1$H NMR line at 1.9 ppm ($\pm 0.1 \cdot 10^{20}$ $g^{-1}$)

Since some of the SAPO-5 samples synthesized contain by-products (spherulitic particles up to about 20 µm in diameter), one could argue that the silicon could be preferentially incorporated not into the AFI phase, but into the by-product. Therefore, we have performed a synthesis under conditions that favour the formation of the by-product. The synthesis product obtained was then separated into the AFI phase and the by-product by simple decantation basing on the large differences in the size of the particles. The $^{29}$Si MAS NMR and DRIFT spectra are given in Fig. 5. Only traces of signals indicating a silicon incorporation are observed in the spectra of the by-product. They can be attributed to a non-perfect separation of the phases. Hence, we can exclude a preferential silicon incorporation into the by-products.

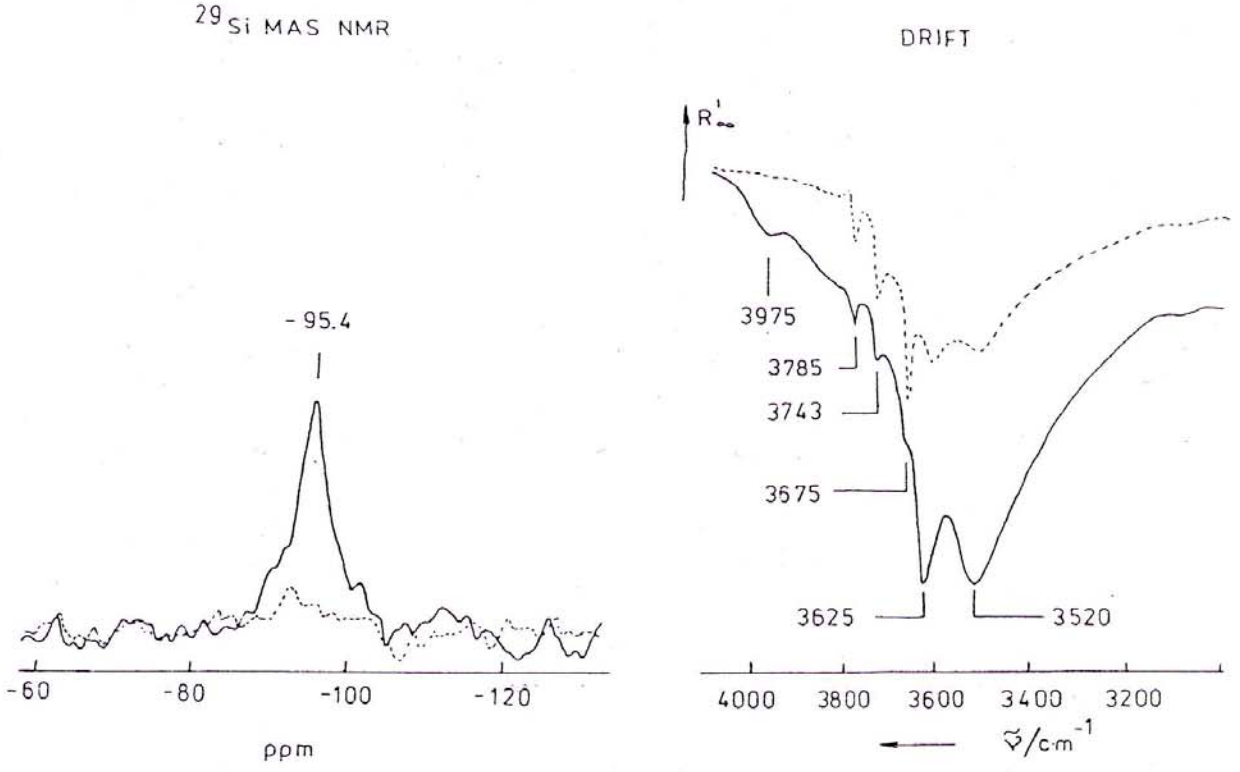


Fig. 5. $^{29}$Si MAS NMR and DRIFT spectra of the by-product (broken lines) and the SAPO-5 phase (solid lines) obtained from the same synthesis batch after calcination.

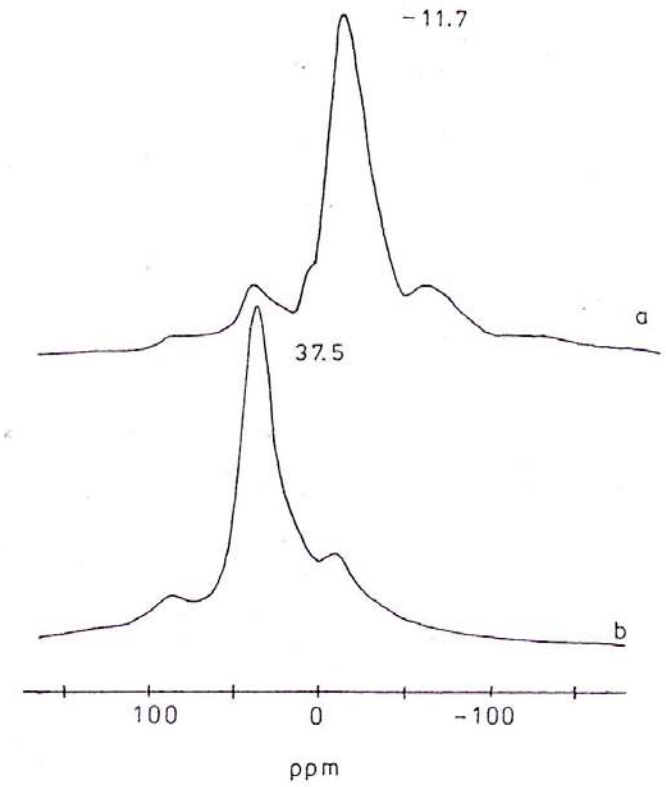


Fig. 6. $^{27}$Al MAS NMR spectra of the by-product:
(a) as-synthesized and (b) calcined and dehydrated.

Concerning the chemical nature of the by-product, we assume that it is an aluminophosphate. This is not only supported by the IR spectrum in Fig. 5, where bands due to AlOH and POH are present, but also by $^{27}Al$ and $^{31}P$ MAS NMR. The line position in the $^{27}Al$ MAS NMR spectrum obtained for the uncalcined by-product (Fig. 6) is characteristic of aluminium in octahedral oxygen coordination in an aluminophosphate (ref. 18). During calcination, the oxygen coordination is changed into a tetrahedral one reflected by a characteristic line position at 37.5 ppm. We failed to assign the by-product to any known aluminophosphate structure by XRD.

## CONCLUSIONS

Morphology and size of the SAPO-5 crystals can be controlled by the composition of the starting gel.

For the crystallization procedure used, a predominant monomeric incorporation of silicon is achieved for quite different crystal morphologies. Well-shaped SAPO-5 crystals containing up to 4% silicon on hypothetical phosphorus T sites can be synthesized.

An upper limit for monomeric incorporation of silicon into SAPO-5 can be expected. Above this limit, only the fraction of silicon present in silica-rich islands within the structure (and/or in amorphous material) is increasing.

The structural changes caused by template removal and by rehydration are not significantly influenced by the incorporation of silicon.

A sometimes obtained by-product of the synthesis was shown to be an aluminophosphate without silicon.

## REFERENCES

1 E.M. Flanigen, R.L. Patton and S.T. Wilson, in: P.J. Grobet, W.J. Mortier, E.F. Vansant and G. Schulz-Eckloff (Eds.), Innovation in Zeolite Material Science, Elsevier, Amsterdam, 1988, pp. 13-28.
2 G. Finger, J. Kornatowski, J. Richter-Mendau, K. Jancke, M. Bülow and M. Rozwadowski, this volume.
3 C. Peuker, G. Finger, E. Löffler and W. Pilz, in preparation.
4 W.M. Meier and D.H. Olson, Atlas of Zeolite Structure Types, 2nd. edn., Butterworths, London, 1987.
5 D. Müller, E. Jahn, B. Fahlke, G. Ladwig and U. Haubenreisser, Zeolites, 5 (1985) 53-56.

6 C.S. Blackwell and R.L. Patton, J. Phys. Chem., 88 (1984) 6135-6139.
7 C.S. Blackwell and R.L. Patton, J. Phys. Chem., 92 (1988) 3965-3970.
8 M. Goepper, F. Guth, L. Delmotte, J.L. Guth and H. Kessler, in: P.A. Jacobs and R.A. van Santen (Eds.), Zeolites: Facts, Figures, Future, Elsevier, Amsterdam, 1989, pp. 857-866.
9 B. Zibrowius, U. Lohse, K. Szulzewsky, H. Fichtner-Schmittler, W. Pritzkow and J. Richter-Mendau, this volume.
10 O.V. Kikhtyanin, V.M. Mastikhin and K.G. Ione, Appl. Catal., 42 (1988) 1-13.
11 D. Freude, H. Ernst, M. Hunger, H. Pfeifer and E. Jahn, Chem. Phys. Lett., 143 (1988) 477-480.
12 E. Brunner, H. Ernst, D. Freude, M. Hunger and H. Pfeifer, in: P.J. Grobet et al. (Eds.), Innovation in Zeolite Materials Science, Elsevier, Amsterdam, 1988, pp. 155-166.
13 J.A. Martens, M. Mertens, P.J. Grobet and P.A. Jacobs, in: P.J. Grobet et al. (Eds.), Innovation in Zeolite Materials Science, Elsevier, Amsterdam, 1988, pp. 97-105.
14 G. Finger, E. Jahn, D. Zeigan, B. Zibrowius, K. Szulzewsky, J. Richter-Mendau and M. Bülow, Bull. Soc. Chim. Belg., 98 (1989) 291-295.
15 I.P. Appleyard, R.K. Harris and F.R. Fitch, Chem. Lett., (1985) 1747-1750.
16 S.G. Hedge, P. Ratnasamy, L.M. Kustov and V.B. Kazansky, Zeolites, 8 (1988) 137-141.
17 C. Halik, J.A. Lercher, H. Mayer, J. Chem. Soc., Faraday Trans. 1, 84 (1988) 4457-4469.
18 D. Müller, I. Grunze, E. Hallas and G. Ladwig, Z. anorg. allg. Chem., 500 (1983) 80-88.